Double-peaked impact force of very soft gel balls

Yoshimi Tanaka
Creative Research Initiative "SOUSEI," Hokkaido University, Kita 21 Nishi 10, Sapporo 011-0021, Japan
(Received 6 November 2005; published 8 March 2006)

We measure the time change of the contact force $F(t)$ during the impact between very soft gel balls and a rigid substrate. For low-impact velocities V_i, $F(t)$ is single-peak functions as intuitively expected; and the relation between V_i and the peak value F_m [of $F(t)$] obeys the prediction of the standard theory for the impact in the linear elastic regime (i.e., the Hertz theory). On the other hand, for large V_i, where the gel ball deforms into thin pancakelike shapes, $F(t)$ becomes double-peak functions. We compare the data of $F(t)$ for large V_i with a prediction of a model proposed in our previous study [Tanaka, Europhys. J. E **18**, 95 (2005)]. The model can quantitatively reproduce the experimental $F_m - V_i$ relation, and shows that the double-peak behavior of $F(t)$ is a consequence of the expanding deformation of the pancake-shaped gel, i.e., spreading motion parallel to the substrate.

DOI: 10.1103/PhysRevE.73.031403 PACS number(s): 82.70.Gg, 61.41.+e, 62.20.Fe, 46.55.+d

I. INTRODUCTION

Impacts of two or more independent bodies are complicated phenomena concerned with a wide range of practical and fundamental problems. Thus, they are still actively studied in the fields of mechanical engineering [1,2], biomechanics [3], and granular [4] and soft matter physics [5,6]. Physically, an impact process can be characterized by the following quantities [1]: (i) the change in the shape of the bodies at the maximum deformation, (ii) the time needed to accomplish the maximal deformation, and (iii) the maximum contact force during the impact. Furthermore, the restitution coefficient is an important (but difficult) quantity from both fundamental and practical points of view [7]. Phenomenologically, understanding the impact of a system is interrelating the above quantities based on an adequate constitutive relation and on reasonable physical simplifications. For the case of the impact between an elastic sphere and a rigid substrate (or between two elastic spheres), the classical Hertz theory provides a theoretical foundation [8,9]. The starting point of the theory is an analytical result for the relation between the *static* contact force F and the indentation Y [see Fig. 1(a)],

$$F = F_H(Y) = \frac{4E}{3(1-\nu^2)} R^{1/2} Y^{3/2}, \tag{1}$$

where R, ν, and E are the radius, Poisson's ratio, and Young's modulus of the sphere, respectively. The corresponding elastic potential U_H is

$$U_H(Y) = \frac{8E}{15(1-\nu^2)} R^{1/2} Y^{5/2}. \tag{2}$$

For the impact of an elastic sphere on the substrate [Fig. 1(b)], it is assumed that the above static relations are valid during the impact process, and that the vertical motion of the mass center is the only relevant mode for the kinetic energy. Under this assumption, the impact is equivalent to the one-dimensional motion of a mass point with the mass $M = (4\pi/3)\rho R^3$ (ρ is the density of the original sphere) confined in the nonharmonic and monotonically increasing potential $U_H(Y)$ [see Fig. 1(c)]; $Y(t)$ and $F(t) = F_H[Y(t)]$ are single-peak functions. The maximal indentation Y_m, the maximal contact force F_m, and the time τ_m needed to accomplish the maximal deformation (hereinafter "deformation time") can be easily obtained, as functions of the impact velocity V_i, from the condition of energy conservation, $\frac{1}{2} M V_i^2 = U_H(Y_m) = M(dY/dt)^2 + U_H(Y)$,

$$Y_m/R = (15\pi/16)^{2/5} (V_i/V_c)^{4/5}, \tag{3}$$

$$F_m/F_c = F_H(Y_m)/F_c = (15\pi/16)^{3/5} (V_i/V_c)^{6/5}, \tag{4}$$

$$\tau_m = \int_0^{Y_m} \frac{dY}{\sqrt{V_i^2 - 2U_H(Y)/M}} = \frac{Y_m}{V_i} \int_0^1 \frac{dz}{\sqrt{1-z^{5/2}}} = 2.26 \times \tau_c \left(\frac{V_i}{V_c}\right)^{-1/5}, \tag{5}$$

where we introduced a characteristic velocity $V_c \equiv \sqrt{E/\rho}$, a characteristic force $F_c \equiv ER^2$, and a characteristic time scale $\tau_c \equiv R/V_c$, and we also set $\nu = \frac{1}{2}$ (incompressibility condition), which is nearly exact for soft polymeric materials. The characteristic powers of $\frac{3}{2}$ in Eq. (1) and other fractional powers in Eqs. (2)–(5) can be directly obtained by a simple scaling argument [10].

For the static contact and the impact of soft polymeric materials, such as rubbers [11,12] and gels [13,14], the physical picture of the Hertz theory breaks down. In particular, it was observed that impacting gel balls deform into thin pancakelike shapes on the rigid substrate; in this case, the maximal lateral dimension R_m (i.e., the maximal radius of the pancake), rather than the maximal indentation Y_m, is the appropriate quantity to characterize the deformation. Experimental data showed that R_m is proportional to V_i, and that τ_m is independent of V_i. These results were qualitatively explained on scaling level by a simple argument that treats the lateral spreading of the gel balls as the principal deformation mode [13]. A simple model assuming uniform and uniaxial

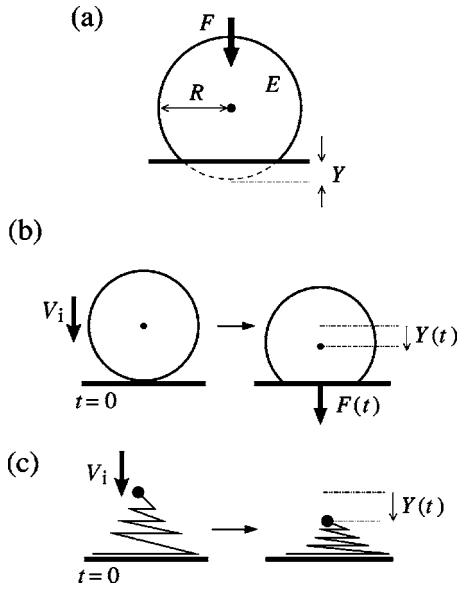

FIG. 1. (a) Static contact between a rigid substrate and an elastic sphere with a radius R and Young's modulus E. (b) An impact of the elastic sphere on the substrate with an impact velocity V_i. (c) A mass-spring model demonstrating the idea of the Hertz theory.

deformation (hereinafter "affine model") quantitatively reproduced the behavior of τ_m without any fitting parameter [14].

In the present study, we experimentally investigate the contact force $F(t)$ for the impact of the gel balls, and compare the experimental result with the prediction of the affine model. For large V_i, the data of $F(t)$ has two peaks, and the maximum contact force F_m (corresponding to the first peak) increased more rapidly with V_i than the prediction of the Hertz theory [Eq. (4)]. The affine model can qualitatively reproduce the data of $F_m(V_i)$, and tells us that the double-peak behavior of $F(t)$ is a consequence of the spreading motion characteristic for the impact of soft materials.

II. EXPERIMENT

The materials (acrylamide gels) and the method to perform the impact experiment are identical with our previous study [13,14]. Spherical acrylamide gels (gel balls), 5 cm in thickness, were synthesized by a standard radical polymerization of acryamide (AAm) monomer and cross-linker of N,N'-methylenebis (acrylamide) (MBAA). The reaction was initiated by ammonium persulpahte and accelerated by tetramethylethylenediamine. By changing the amounts of the feed molecules (AAm and MBAA), we obtained four kinds of sample gels with different mechanical properties. Hereafter, we use the abbreviation of "AxBy" (x and y are numbers) to indicate each of them; AxBy gel has the following composition of solvent, monomer and cross-linker: 100 g of water; x g of AAm; $\left(\frac{1}{100}\times y\right)$ g of MBAA. Rheological characterization of the sample gels revealed that they behave as elastic materials in the frequency range from 0.1 to 100 Hz, i.e., the real part of the complex Young's modulus, E', hardly depends on the frequency, and tan δ has very small values (tan $\delta < 0.01$ for A10B30 gel and tan $\delta \approx 0.07$ even for the most lossy A10B4 gel). E' at 50 Hz (regarded as the normal Young's modulus E) and the characteristic velocity $V_c \equiv \sqrt{E/\rho}$ are presented in Table I.

TABLE I. Young's modulus E and a characteristic velocity $V_c \equiv \sqrt{E/\rho i\rho}$ is density of the sample gels). The values of E was determined, from rheological measurements, as the real part of the complex Young's modulus at 50 Hz.

Sample name	$E(10^4$ Pa)	V_c (m/s)
A6B6	0.61	2.40
A10B4	1.24	3.42
A10B15	3.88	6.05
A10B30	6.46	7.81

The impact experiment was performed by using free fall; the impact velocity V_i was determined by the relation of $V_i = \sqrt{2gh}$, where h is the height at which the gel balls begin to fall down, and $g = 9.8$ m/s^2 is the acceleration of gravity. The substrate on which the spherical gels impact had a sandwich structure made of a circular aluminum plate (lower plate, 1 cm in thickness and 25 cm in diameter), three force gauges to measure the contact force during the impacts (LMA-100N, Kyowadengyo Co.), and a circular acrylate resin plate (upper plate to directly receive the impact of the gel balls, in the same dimensions as the lower aluminum plate). The aluminum plate was fixed onto the floor with bolts, and the gauges were glued to the plates with double-faced adhesive tape. The contact force $F(t)$ acting on the gauges during the impacts was monitored and recorded with a DC type strain amplifier (AS 2503, NEC Sanei Co.) and a digital oscilloscope (DS-4264M, IWATSU Co.) connected to the amplifier. The deformation processes of the gel balls were recorded with a high-speed video camera (Motion Coder Analyzer, Kodak Co.).

III. RESULTS

Figures 2(a)–2(d) show the time change of the contact force $F(t)$ and the corresponding deformation processes at different (reduced) impact velocities. In the $F(t)$ graphs, the jagged curves show the original data (the sampling interval is 2×10^{-2} ms). The curves contain oscillatory components with a typical peak-to-peak period of 1 ms. These components, probably coming from vertical oscillation of the acrylate resin plate due to a finite stiffness of the force gauges, made it difficult to determine the peak value F_m of the *true* contact force; we smoothed the original data by moving average over an averaging time of 2.4 ms. The averaging time is such that the oscillation components of $F(t)$ are smoothed out, but that whole shape of $F(t)$ is unchanged. Hereafter, $F(t)$ indicates the averaged data. In each sequential pictures below the $F(t)$ graph, the first, third, and last pictures show the gel at the initial contact, the maximal deformation and the "taking-off," respectively.

Figure 2(a) shows the experimental results at $V_i/V_c = 0.26$. $F(t)$ is a single-peak function. The shape of $F(t)$ is

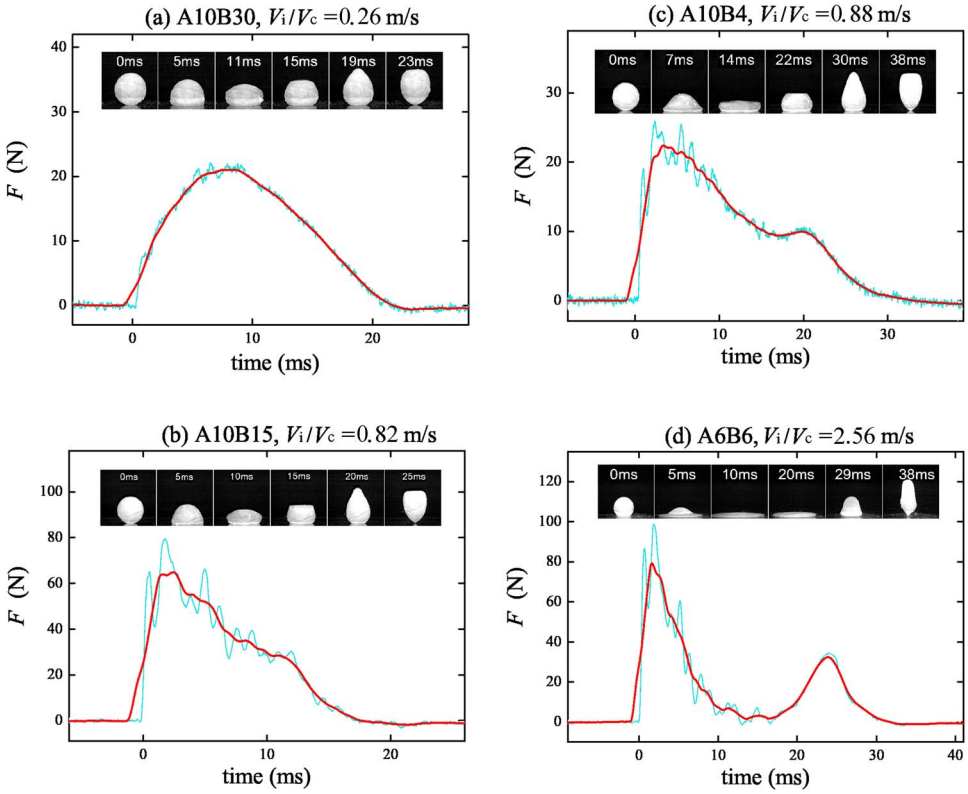

FIG. 2. (Color online) Time change of the contact force $F(t)$ and the corresponding impact process (lower sequential pictures). (a) A10B30 gel, V_i=2.0m/s, V_i/V_c=0.26. (b) A10B15 gel, V_i=5.0m/s, V_i/V_c=0.82. (c) A10B4 gel, V_i=3.0m/s, V_i/V_c=0.88. (d) A6B6 gel, V_i =6.0m/s, V_i/V_c=2.56. In the graphs of $F(t)$, the jagged curves are the original data, and the thick curves are obtained by performing moving average of the original data over an averaging time of 2.4 ms. In each deformation process, the third picture shows the shape of the gel ball at the maximal deformation.

somewhat asymmetrical about the peak position, corresponding to the asymmetrical deformation process. For V_i/V_c =0.66, a small shoulder appears after the peak of $F(t)$ (the data is not presented); and for V_i/V_c=0.82 [Fig. 2(b)], the shoulder becomes distinct [see the $F(t)$ curve around t =0.012 s]. For V_i/V_c=0.88, a *secondary peak* appears in $F(t)$ as shown in Fig. 3(c). For V_i/V_c=2.56, where the gel ball remarkably flattens, $F(t)$ completely separates into two "hill" between which $F(t)$ falls to near zero [Fig. 2(d)].

Figure 3 is a plot of the peak value F_m [of $F(t)$] versus V_i. F_m and V_i are nondimensionalized with the characteristic quantities F_c ($\equiv ER^2$) and V_c ($\equiv\sqrt{E/\rho}$), respectively. We regard the range of $0.66<V_i/V_c<0.82$ (shaded in Fig. 3), where the shoulder appears in $F(t)$, as the crossover region from the single-peak to the double-peak behavior of $F(t)$. Above the crossover regime, both the first and the secondary peak forces are plotted. The data points from the different gels fall onto the single behavior. The data of F_m is in agreement with the prediction of the classical Hertz theory [Eq. (4)] at low impact velocities ($V_i/V_c<1$); while, for higher V_i/V_c, the data exceeds the Hertz curve, and agrees with the prediction of our model described in the next part.

IV. COMPARISON WITH AFFINE DEFORMATION MODEL

In this section, we compare the experimental result of the impact force with the prediction of the model proposed in Ref. [14]. The model assumes that (i) after the onset of an impact, a gel ball uniformly deforms into ellipsoidal shapes, keeping the symmetry about the vertical line passing through the center of the ball and about the horizontal plane containing the center (Fig. 4), that (ii) the neo-Hookean (ideal rubber-type) elastic energy applies to the gel ball, and that (iii) the gel ball is incompressible.

Thanks to the assumption (i), motion and deformation of the gel ball can be characterized by elongation ratios for the vertical direction α and for the lateral direction β as shown in Fig. 4: the vertical velocity $V(t)$ of the mass center is given by $R\dot{\alpha}$; and a material point of (x,y,z) [(x,y,z) is the Lagrange coordinate relative to the center] moves to the relative position of $[\beta(t)x,\beta(t)y,\alpha(t)z]$ at a given time t. The incompressibility condition (iii) provides a constraint between α and β, $\alpha(t)\beta(t)^2=1$. The dynamics of the system is determined by the following Lagrangian of a pair of harmonic oscillators α and β coupled by the incompressibility condition [14]:

$$L=\left(\frac{m_\alpha}{2}R^2\dot{\alpha}^2+\frac{m_\beta}{2}R^2\dot{\beta}^2\right)-\frac{1}{2}\frac{EM}{3\rho}(\alpha^2+2\beta^2-3), \quad (6)$$

$$\alpha(t)\beta(t)^2=1, \quad (7)$$

where $m_\alpha\equiv 6M/5$ and $m_\beta\equiv 2M/5$. The first term is the kinetic energy, which was calculated as the sum of

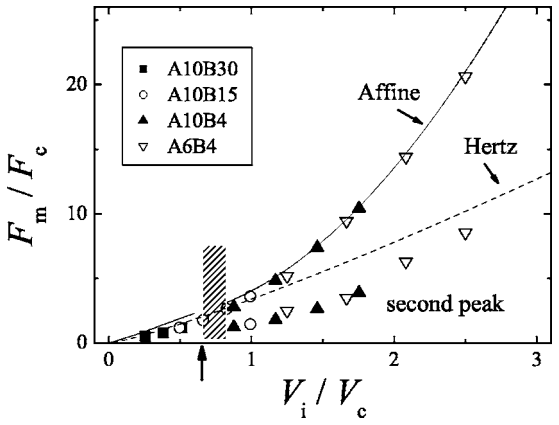

FIG. 3. A plot of the peak contact force F_m/F_c vs the reduced impact velocity V_i/V_c. The prediction of the Hertz theory and that of our model are represented together (denoted as Hertz and Affine, respectively).

$\frac{1}{2}M(R\dot{\alpha})^2$ (due to the translational motion of the mass center) and $\int(\rho/2)(\dot{\alpha}^2z^2+\dot{\beta}^2x^2+\dot{\beta}^2y^2)dxdydz=\frac{1}{2}(M/5)R^2\dot{\alpha}^2+\frac{1}{2}(2M/5)R^2\dot{\beta}^2$ (due to the internal deformation). The second term is the potential energy; we employed the neo-Hookean deformation energy according to (ii) (see, for example, Ref. [15] for details of the deformation energy). The terms of

$$K_\alpha \equiv \frac{m_\alpha}{2}R^2\dot{\alpha}^2 \text{ and } K_\beta \equiv \frac{m_\beta}{2}R^2\dot{\beta}^2 \tag{8}$$

in Eq. (6) can be regarded as the kinetic energies due to the vertical and to the lateral (spreading) motions, respectively, and m_α (m_β) is the "effective mass" for the vertical (lateral) direction.

Eliminating β and $\dot{\beta}$ ($\beta=\alpha^{-1/2}$ and $\dot{\beta}=-\alpha^{-3/2}\dot{\alpha}/2$) and using the Euler-Lagrange equation $(d/dt)(\partial L/\partial\dot{\alpha})-(\partial L/\partial\alpha)=0$, we obtain the equation of motion for α,

$$\alpha'' + f(\alpha)\alpha'^2 + g(\alpha) = 0, \tag{9}$$

$$f(\alpha) \equiv -\frac{3}{2\alpha(12\alpha^3+1)}, \quad g(\alpha) \equiv \frac{10(\alpha^4-\alpha)}{3(12\alpha^3+1)}, \tag{10}$$

where we used the nondimensional time $s \equiv t/\tau_c$ as the argument of α, and the prime symbol $'$ represents the differential with respect to s. Initial conditions are

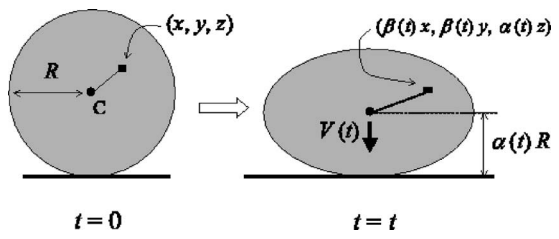

FIG. 4. Deformation assumed in the affine deformation model. A material point (x,y,z) moves to $(\beta(t)x, \beta(t)y, \alpha(t)z)$.

$$\alpha(0) = 1 \text{ and } \alpha_0' (\equiv \alpha'(0)) = \sqrt{\frac{10}{13}}\frac{V_i}{V_c}. \tag{11}$$

The condition for α_0' comes from the requirement of energy conservation at $t=0$, $\frac{1}{2}MV_i^2 = (K_\alpha+K_\beta)|_{t=0}$ [14]. It should be noticed that Eq. (9) is invariant for the variable transformation of $s \to -s$, i.e., the system fulfills the time reversibility.

In Fig. 5, we present predictions of the model on $\alpha(s)$ and $\alpha''(s)$ for different V_i/V_c, determined from numerical solutions of Eqs. (9)–(11). $\alpha''(s)$ is proportional to the contact force of the model gel ball, because the vertical position of the mass center is $R\alpha$, and the contact force is given by $F=MR\ddot{\alpha}=(4\pi/3)F_c\alpha''$. At first view, the shape of the $\alpha''(s)$ curve is fairly different from the experimental data shown in Fig. 2: the curves of $\alpha(s)$ and $\alpha''(s)$ have symmetrical shapes about the time at which α arrives at the minimum because of the time reversibility of Eq. (9); on the other hand, the actual impact force $F(t)$ is quite asymmetrical in time. However, the affine model grasps interesting characteristics of the data. Firstly, the model predicts that the peak splitting of $F(t)$ occurs at an intermediate V_i/V_c (in the next paragraph, we describe the critical impact velocity for the splitting in detail), and that for large V_i/V_c, $\alpha''(s)$ falls to near zero between the two peaks. Secondly, the model can reproduce the maximum value of the contact force F_m; in Fig. 3, we present the prediction of the model on the relation between F_m/F_c and V_i/V_c. (For the affine model, the second peak force is identical to the first one because of the time reversibility.) The prediction is in good agreement with the experimental behavior of F_m for the first peak.

For the affine model, the *critical impact velocity* V_i^*, above which $\alpha''(s)$ becomes a double-peak function, can be determined as follows. Let us denote the solution of Eq. (9) with V_i^* as $\bar{\alpha}(s)$, and the (scaled) time at which $\bar{\alpha}$ arrives at the minimum as s^*. The two maxima and the minimum of $\alpha''(s)$ for $V_i > V_i^*$ merge at the point of $[s^*, \bar{\alpha}(s^*)]$ of the $s-\alpha$ plane; thus, we have the following condition to determine $\bar{\alpha}^* \equiv \bar{\alpha}(s^*)$:

$$\bar{\alpha}'(s^*) = \bar{\alpha}'''(s^*) = \bar{\alpha}''''(s^*) = 0. \tag{12}$$

With these conditions, Eq. (9) reduces to $\bar{\alpha}''(s^*)+g(\bar{\alpha}^*)=0$, and the twice differential of Eq. (9) to $2f(\bar{\alpha}^*)\bar{\alpha}''(s^*)+(\partial g/\partial\alpha)(\bar{\alpha}^*)=0$. Combining these relations, we have the equation to determining $\bar{\alpha}^*$, $2f(\bar{\alpha}^*)g(\bar{\alpha}^*)-(\partial g/\partial\alpha)(\bar{\alpha}^*)=0$. The numerical solution of this equation is $\bar{\alpha}^*=0.497$, and the critical impact velocity V_i^* can be obtained from the energy conservation at $s=s^*$, $\frac{1}{2}MV_i^{*2}=\frac{1}{2}(EM/3\rho)(\bar{\alpha}^{*2}+2/\bar{\alpha}^*-3)$ [the r.h.s. is the potential term of Eq. (6)], resulting in $V_i^*/V_c=0.65$. This value of V_i^*/V_c is marked in Fig. 3 with the upward arrow. The critical value of V_i/V_c is consistent with the crossover regime of the experimental data.

In summary, the affine model can reproduce the double-peak behavior of the contact force $F(t)$ for large V_i/V_c, and can make a qualitative prediction on the dependence of the maximal (i.e., the first peak) contact force F_m on the impact velocity.

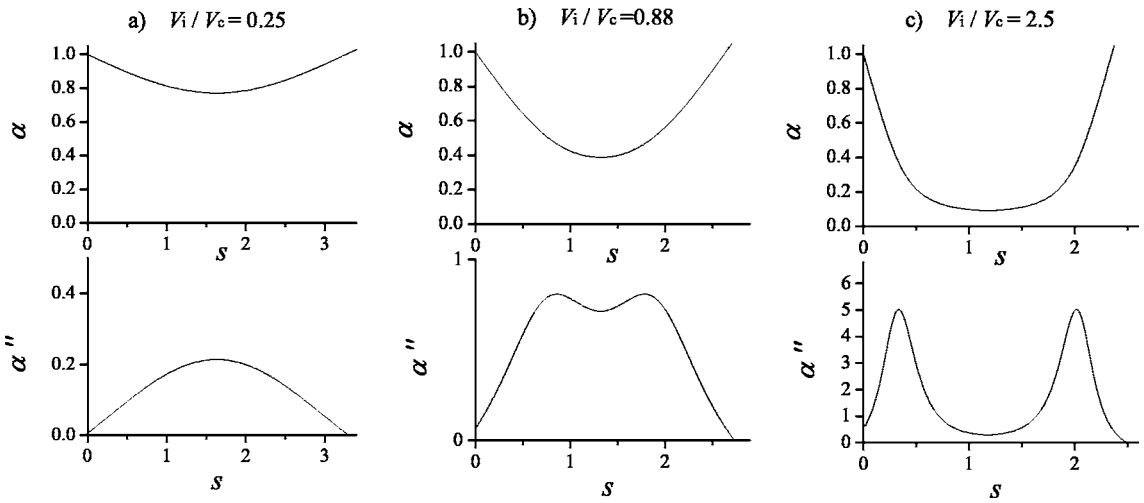

FIG. 5. Predictions of the affine model on $\alpha(s)$ and $\alpha''(s)$.

V. DISCUSSION

We give an intuitive explanation for the double-peak behavior of $F(t)$. Although the following argument is based on the affine model, the conclusion holds for the actual impact. We consider the large impact velocity regime, where the curve of $\alpha(s)$ has a bucketlike shape, i.e., the shape with a broad bottom and tilt walls, as seen in Fig. 5(c). If we accept the shape of the curve, the double-peak behavior of α'' can be intuitively understood by considering osculating circles at each part of the $\alpha(s)$ curve (the curvature, roughly proportional to α'', is large only around the feet of both the walls). Thus, what we should do here is to make an intuitive explanation for the characteristic shape of the $\alpha(s)$ curve: For a large impact velocity, the gel ball rapidly decreases its vertical dimension after the initial contact; this period corresponds to the left wall. Then, the deformation arrives at such a state that the vertical dimension is sufficiently small ($\alpha \ll \beta$), but the gel ball has a nonzero kinetic energy, most of which is accounted for by K_β (because $|\dot{\alpha}| \ll |\dot{\beta}|$). After that, β increases toward the maximal deformation, transferring the energy from K_β to the potential term $(EM/2\cdot 3\rho)\beta^2$, while α remains at small values for a while. This period corresponds to (the left half of) the broad bottom. After the maximal deformation, α changes in the reverse way, forming the right half of the bucket. It should be noticed that the double-peak behavior is governed by the energy exchange between K_α and K_β, the former is due to the vertical motion of the mass center, the latter to lateral (spreading) motion.

The essence of the above argument is the stagnation of the mass center position due to the flattening and to the redirection of the velocity of each part of the gel; the existence of the kinetic energy due to the lateral (spreading) motion plays a crucial role. Therefore, the mechanism applies to the impact of actual gel balls, and to the impact of a wider range of soft materials that can undergo large deformation without breaking, such as small water drops on super hydrophobic substrate [5,6].

Lastly, we discuss on the origin of the asymmetry in the experimental behavior of $F(t)$, which cannot be explained by the affine model. There are two candidates for the origin: (i) dissipative events due to bulk viscosity and friction between the gel balls and the substrate (the substrate is normally dried in this study, i.e., not treated with any lubricant liquid, see below), and (ii) nonuniform deformations of the gel balls due to the asymmetrical boundary condition [14], that is, as seen in Fig. 2, the upper parts of the ball is strongly tipped up after the maximal deformation, while the acceleration of the mass center is delayed and tardy. Actually, the dissipative events give very minor effects on the impact behavior, and thus the asymmetry of $F(t)$ is attributed to (ii). This is because (1) the viscoelastic (rheological) measurements revealed that all gels used in the experiment have very low values of tan δ (≈ 0.07 even for the most dissipative A10B4 gel) at the frequencies relevant to the impact experiment (~ 100 Hz), and because (2) control experiment on the impacts with the slippery substrate (gotten wet with a low viscosity oil or solution of surfactant) showed no remarkable difference of the impact behavior (the deformation time, etc.). To deal with the irreversible elastic deformation, we need to extend the affine model by adding other degrees of freedom that express the asymmetry of the deformation.

ACKNOWLEDGMENTS

The author thanks K. Okumura, J. P. Gong, and M. Matsushita for their kind support. He also thanks T. Kurokawa for his assistance with measurements, and the Institute of Science and Engineering at Chuo University for financial support.

[1] W. Goldsmith, *Impact* (Arnold, London, 1960).
[2] R. Sburlati, J. Compos. Mater. **36**, 1079 (2002).
[3] N. Shewchenko, C. Withnall, M. Keown *et al.*, Br. J. Sports Med. **39**, I10 (2005).
[4] C. Daraio, V. F. Nesterenko, E. B. Herbold, and S. Jin, Phys. Rev. E **72**, 016603 (2005).
[5] K. Okumura, C. Clanet, D. Richard, and D. Quéré, Europhys. Lett. **62**, 237 (2003).
[6] C. Clanet, C. Béguin, D. Richard, and D. Quéré, J. Fluid Mech. **517**, 199 (2004).
[7] H. Hayakawa and H. Kuninaka, Chem. Eng. Sci. **157**, 239 (2002) and references therein.
[8] H. Hertz, J. Reine Angew. Math. **92**, 156 (1882).
[9] D. Maugis, *Contact, Adhesion and Rupture of Elastic Solids* (Springer, New York 2000).
[10] P. G. de Gennes, Europhys. Lett. **35**, 145 (1996).
[11] Y. Tatara, J. Eng. Mater. Technol. **105**, 67 (2003).
[12] Y. Tatara, J. Eng. Mater. Technol. **113**, 285 (1991).
[13] Y. Tanaka, Y. Yamazaki, and K. Okumura, Europhys. Lett. **63**, 149 (2003).
[14] Y. Tanaka, Eur. Phys. J. E **18**, 95 (2005).
[15] G. R. Strobl, *The Physics of Polymers* (Springer-Verlag, Berlin, 1997).